Tellus (1980), *32*, 6–14

An observational study of the upward sensible heat flux by synoptic-scale transients

By J. OERLEMANS, *Royal Netherlands Meteorological Institute, Postbus 201, 3730 AE De Bilt, The Netherlands*

(Manuscript received June 21; in final form October 5, 1979)

ABSTRACT

For eight 30-day periods, two in each season, vertical transient eddy fluxes of sensible heat were computed at the 850, 500 and 200 mb levels. Use was made of NMC analyses and 6-h forecasts of the ω-field available twice a day.

Vertical heat fluxes are strong in the Atlantic and Pacific storm track, and over Scandinavia and Canada. The conversion of potential to kinetic energy (which is directly related to the upward sensible heat flux) by the synoptic scale transients, averaged over the whole atmosphere north of 20° N, shows maxima in spring (2.6 W m^{-2}) and fall (2.2 W m^{-2}). Summer and winter show lower conversion rates (1.2 and 2.1 W m^{-2}, respectively). The yearly conversion amounts to 2.0 W m^{-2} which is in good agreement with the value of 2.2 W m^{-2} obtained by Oort and Peixoto (1974). Their estimate includes standing eddies, however.

We find that the zonal mean vertical and northward sensible heat fluxes are strongly coupled. The parameterization $\overline{\omega' T'} = \mu \overline{v' T'}$ is tested both with regard to latitude and season. It appears to perform quite well with $\mu = -1.5 \times 10^{-4}$ to -2×10^{-4} m mb^{-1}.

1. Introduction and background

In budget studies of the general circulation of the atmosphere, terms involving vertical motion have always acted as obstacles. The reason is well known: it is impossible to measure them, at least on the synoptic and planetary scale. In spite of this handicap, several attempts have been made to estimate vertical eddy transports. A technique frequently used is that of closing a budget, that is, solving the vertical eddy flux from a time- and/or longitude-averaged equation that states the conservation of the quantity in question. An example of this approach is the study by Hantel (1976). Concerning the energy budget, difficulties arise because no distinction can be made between dissipation and eddy energy conversion. A second method to derive vertical eddy transports is to estimate the vertical motion by a kinematic procedure using upper air wind measurements (Kung, 1972), but this makes sense only in regions with a dense upper air network.

Still another approach is to make use of vertical motion fields computed with a hydrodynamical model, preferably including orography and diabatic heating. Such a method may be called a "quasi-observational" method. Examples are the studies by Berggren and Nyberg (1967) and Lau (1979). The easiest way to compute vertical motion fields is to employ a quasi-geostrophic model because it carries a simple diagnostic equation for $\omega(=dp/dt)$. However, as stressed by Holopainen (1963) and others, a quasi-geostrophic model is not very suitable for energy conversion calculations. In principle, primitive equation models should give the best results. The vertical motion is computed by integration of the continuity equation with respect to pressure, which at present seems to be the best procedure.

In this paper, vertical fluxes of sensible heat at the 850, 500 and 200 mb levels will be presented, computed according to the last method. The temperature and vertical motion fields used were produced by the National Meteorological Center (U.S.A.). They are stored in the data archive of NCAR where all computations were carried out.

The relevance of studying the vertical sensible heat flux is twofold. First, it is important from a

0040-2826/80/010006–09$02.50/0

modelling point of view because $\overline{\omega' T'}$ appears in the time-averaged thermodynamic equation. Diagnostic studies of $\overline{\omega' T'}$ may help to parameterize this term for use in statistical-dynamical models.

Second, $-\overline{\omega' T'}$ is related to the vertical mass flux by the ideal gas law, i.e.

$$-\overline{\omega' \alpha'} = -\frac{R}{p_0}\overline{\omega' T'} \tag{1}$$

and may therefore be interpreted as a conversion of potential into kinetic energy. For a discussion of the differences between the so-called $\omega\alpha$-formulation (used in this study) and the $\mathbf{V}\cdot\nabla\phi$-formulation of the energy conversion, see e.g. Hantel and Baader (1976) and Oort and Peixoto (1974). Here we recall that those formulations should give the same result if the conversion is averaged over a large part of the atmosphere, i.e. so large that fluxes of energy through the boundaries can be neglected.

Unless stated otherwise, symbols have their usual meaning. A bar always denotes a 30-day mean value, a prime the deviation from this value. The symbol $\langle\ \rangle$ refers to a zonal average. Vertical, hemispheric and seasonal mean values will be explicitly mentioned when they appear.

2. Data source and processing

All data used were extracted from NMC material. Among other quantities, this material provides temperature fields twice a day (at 00 and 12 GMT) at the standard pressure levels. Concerning vertical motion fields, only 6-h forecasts were available (for 06 and 18 GMT). This is because, regardless of the details of the initialization method, a sufficiently accurate balance between wind and mass fields is established after 6 h of integration. The NMC forecast model used to compute the ω-fields is a six-layer primitive equation model formulated in σ-coordinates, so orographic effects are implicitly taken into account. The most important diabatic heating mechanisms are also incorporated. A description of the basic model can be found in Shuman and Hovermale (1968). During the period from which the data were taken (1976 and 1977), the model did not undergo significant changes.

Table 1. *The 30-day periods used in this study. WI, SP, SU and FA denote winter, spring, summer and fall, respectively*

Acronym	Date
WI1	Jan. 7 76–Feb. 5 76
WI2	Dec. 18 76–Jan. 16 77
SP1	Mar. 13 76–Apr. 11 76
SP2	Mar. 26 77–Apr. 24 77
SU1	June 18 76–July 17 76
SU2	June 6 77–July 5 77
FA1	Sep. 28 76–Oct. 27 76
FA2	Oct. 16 77–Nov. 14 77

Eight periods of 30 days (60 analyses) were selected in such a way that there were two periods in each season and no fields were missing. The periods are listed in Table 1. The region considered is the part of the Northern Hemisphere north of 20° N, represented on the well-known NMC grid.

Several ways of dealing with the ω-fields are possible. One may consider the 6-h forecast as being the ω-field 6 h earlier, thus simply shifting them back in time. An alternative is to interpolate the ω-fields to 00 and 12 GMT [$\omega_i = \frac{1}{2}(\omega_{i-6} + \omega_{i+6})$, where i = 00 or 12 GMT], or to interpolate the T-fields to 06 and 18 GMT [$T_{i+6} = \frac{1}{2}(T_i + T_{i+12})$]. As shown below, the difference between those two ways of interpolation is negligible. We my write down expressions for the upward heat flux with interpolated ω-fields and with interpolated T-fields. Subtracting one expression from the other then gives the difference between the methods. Indicating interpolated quantities with an asterisk we find

$$\overline{\omega_{i+6} T^*_{i+6}} - \overline{\omega^*_i T_i} = \tfrac{1}{2}(\overline{\omega_{i-6} T_i} - \overline{\omega_{i+6} T_{i+12}}) \tag{2}$$

The right-hand side contains no fields obtained by interpolation, so eq. (2) expresses the difference in covariance obtained by the two methods in the original fields. Since the covariance will change only slightly if the sample (consisting of 60 points in time) is shifted one point along the time axis, we see that the difference should be very small.

In this study, the ω-fields were interpolated to 00 and 12 GMT. Some sample calculations were carried out to investigate the effect of interpolation. Fig. 1 shows zonal mean values of $\overline{\omega'^2}$ and $\overline{\omega' T'}$ for a 30-day period obtained by the

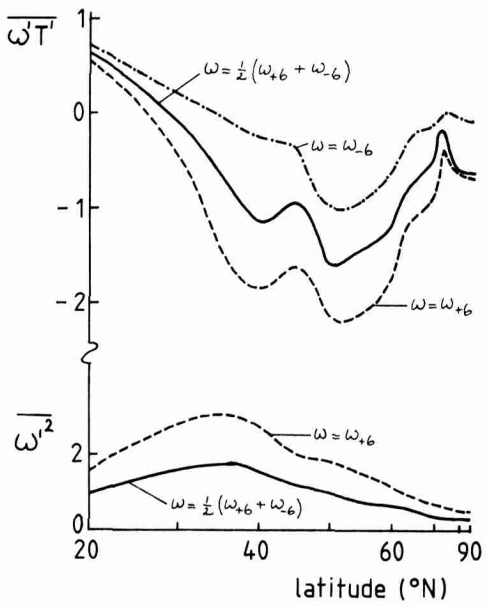

Fig. 1. Zonal mean values of $\overline{\omega'^2}$ and $\overline{\omega' T'}$ obtained by different ways of handling the ω-field. Units are 10^{-3} K · mb s^{-1} and 10^{-6} mb^2 s^{-2}. Curves shown apply to the 500 mb level.

different methods. We first note that interpolation reduces $\overline{\omega'^2}$ about 40%. Thus variations in ω with a time scale smaller than say 36 h, but resolved by the forecast model, contribute considerably to the total variance. In addition, $\overline{\omega' T'}$ appears to be very sensitive to whether interpolation is employed or not. Shifting the ω-field 6 h forward in time (i.e. using ω_{-6}) results in much larger values of $\overline{\omega' T'}$ than shifting the ω-field back (i.e. using ω_{+6}). Interpolation gives values in between, of course. This picture indicates that in synoptic disturbances the ω-field lags the T-field, which is in agreement with baroclinic wave theory (Holton, 1972).

Using interpolated ω-fields, the artificial reduction of $\overline{\omega'^2}$ cannot be avoided. Since we do not know the correlation between ω and T on the time scales that are smoothed out, it is impossible to make any corrections. If the correlation is independent of frequency, the best estimate would be

$$\overline{\omega' T'} = \overline{\omega'_{\text{int}} T'} \, [\overline{\omega'^2_{+6}} / \overline{\omega'^2_{\text{int}}}]^{1/2} \approx 1.3 \overline{\omega'_{\text{int}} T'} \qquad (3)$$

On the other hand, if the correlation on the time scales smaller than 36 h is negligible, $\overline{\omega'_{\text{int}} T'}$ must be the best estimate. It is by no means clear which estimate is preferable. In this study, values of $\overline{\omega'_{\text{int}} T'}$ are given. A fortunate condition is the fact that interpolation has the same effect all over the Northern Hemisphere, at least for the sample calculations carried out. We may therefore expect the geographical distribution of $\overline{\omega' T'}$ to contain a smaller error than its absolute value.

3. Geographical distributions of the upward sensible heat flux

Since 500-mb vertical velocities are supposed to be most reliable, we focus on this level. Fig. 2 shows geographical distributions of $-\overline{\omega' T'}$ at 500 mb for each season and for the entire year. Seasonal values are computed by averaging over the two appropriate periods (see Table 1). The annual mean flux is the average over all samples.

In winter we find three regions where the fluxes are large: the Scandinavian region, the Pacific storm track, and a wide area from the Rocky Mountains to Iceland. During spring and fall the pattern is roughly the same. In summer $-\overline{\omega' T'}$ is much smaller, the major part of the flux taking place over the northern American continent and mid-Siberia.

A striking feature is the large upward heat flux in spring and fall. It appears to be even higher than in winter. All 30-day periods showed this feature, so it can hardly be regarded as a mere sampling effect. We will discuss this point again in the next section.

The patterns of $-\overline{\omega' T'}$ at 850 mb (not shown) appeared to be rather similar to those at 500 mb. In mountainous regions it is not quite clear what $-\overline{\omega' T'}$ represents. Because of this difficulty we will discuss the 850 mb flux in terms of zonal mean values only. The 200 mb flux did not show much correlation with the 500 mb flux. The variation with longitude appeared to be small and rather noisy. The variation with latitude, however, showed a very consistent picture: an upward flux south of the 45° N latitude circle and a downward flux north of it. Therefore, it is also adequately described by zonally averaged values. We turn to this in the next section.

Recently, Lau (1979) computed the geographical distribution of $\overline{\omega' T'}$ for winter, defined as the 120-day period starting from November 15. The agreement between Lau's distribution (given at 700 mb) and the present one is rather good. Differences can be attributed to the different sampling.

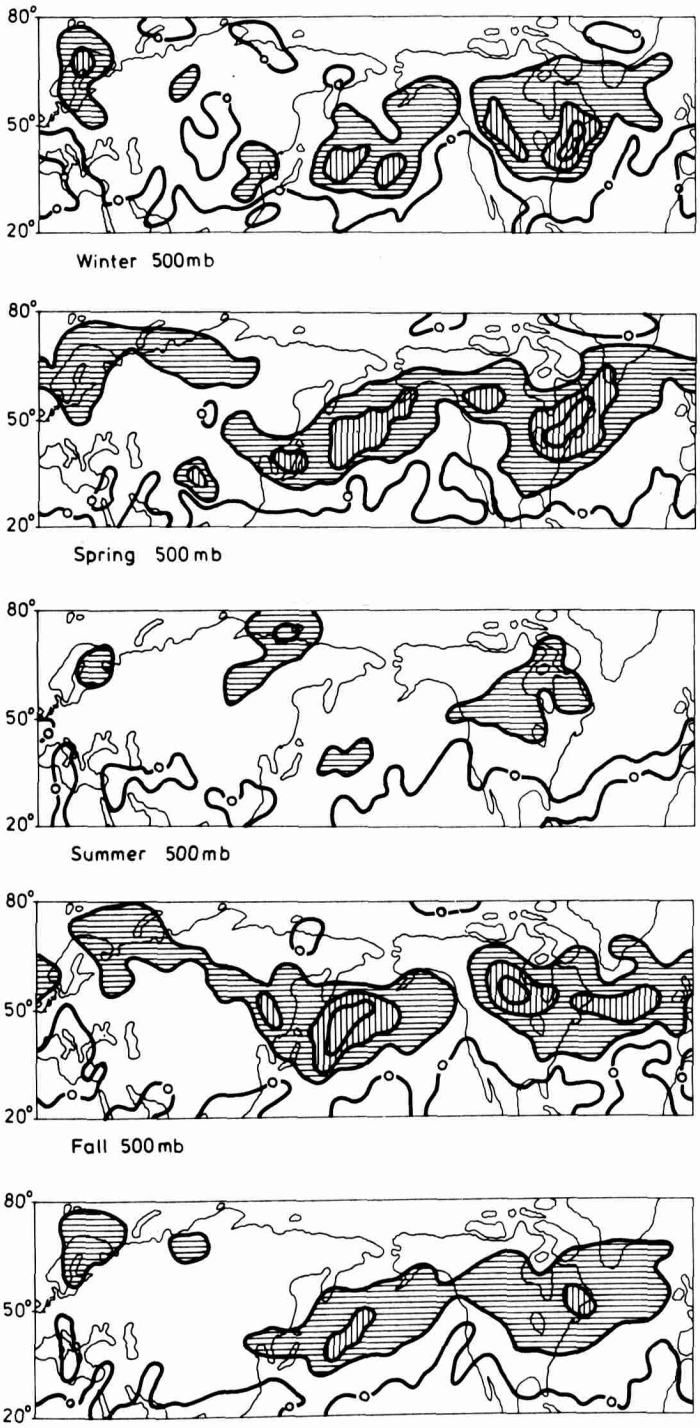

Fig. 2. Upward eddy flux of sensible heat ($-\overline{\omega' T'}$) at 500 mb. Contour interval is 1.5×10^{-3} K · mb s^{-1}. Horizontal and vertical hatching denote regions where the upward flux exceeds 1.5×10^{-3} and 3×10^{-3} K · mb s^{-1}, respectively.

4. Zonal and hemispheric mean values

In the following, we denote zonally averaged values of the upward sensible heat flux by H_i, where the index i is 20, 50 or 85 according to the pressure level involved.

Fig. 3 presents values of H_{20}, H_{50} and H_{85}. The large values of H_{50} during spring and fall come out very sharply. The same may be said of H_{85}, which is strongly correlated with H_{50}. In summer, H_{50} takes on its highest values in high latitudes (around 70° N). Winter and spring show rather flat distributions in contrast to fall, when a sharp peak in H_{50} appears at a latitude of 50° N.

H_{20} shows a very regular dependence on latitude. In the subtropics, H_{20} is positive throughout the year, though in summer values are very small. At high latitudes H_{20} is negative, so potential energy is built up by the eddies. The latitude where H_{20} changes sign approximately coincides with the latitude where the tropopause intersects the 200 mb level. We should keep in mind, however, that it is not clear how strong this "observational" result depends on the representation of the tropopause in the forecast model used to compute the ω-fields.

In order to estimate the eddy energy conversion C_i, we multiply H_i by R/p_i, where R is the gas constant for dry air and p_i the pressure of the level considered. Table 2 presents values of C_i averaged over the entire domain, i.e. the region north of 20° N. The last column gives an estimate of the vertically integrated conversion. For the total yearly mean conversion we find 2.03 W/m^2. This compares very well with the value of 2.2 W/m^2 given by Oort and Peixoto (1974), who obtained this value as a residue from the balance equations for kinetic and potential energy. Their value for January (3.4 W/m^2) is considerably larger than the 2.13 W/m^2 we find for winter, but the values for July (summer) do not differ very much (1.5 and 1.23 W/m^2, respectively). It should be noted that Oort and Peixoto's estimate also contains standing eddies, which reach their largest amplitude in winter.

The result that the yearly mean conversion as estimated by Oort and Peixoto and as computed in

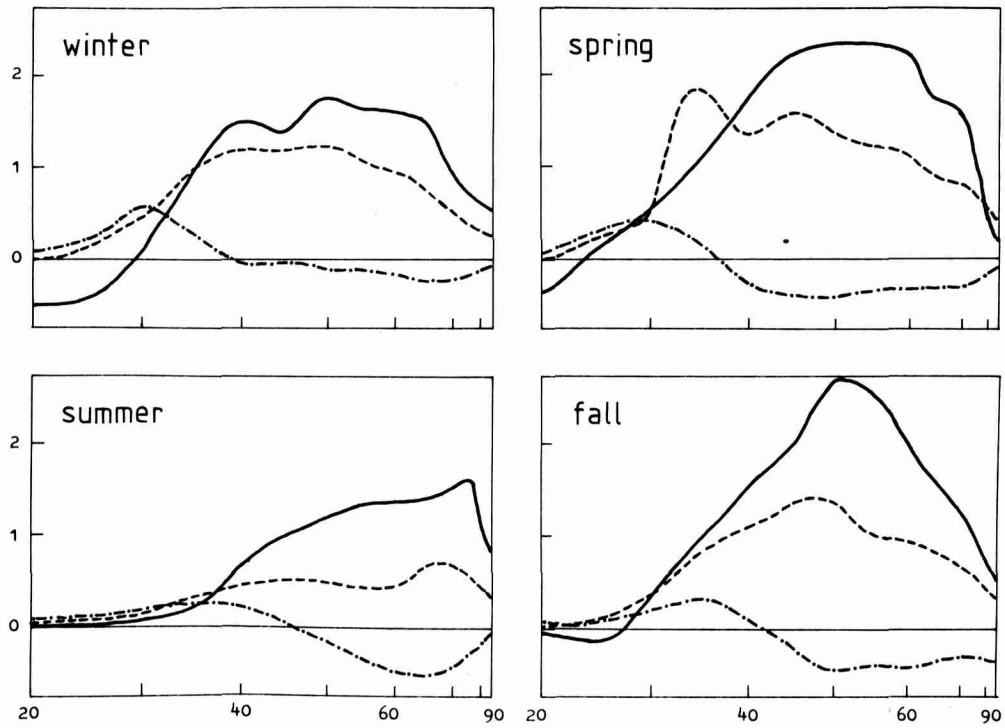

Fig. 3. Zonal mean values of H at the 850 (dashed), 500 (solid) and 200 (dot-dashed) mb levels, as a function of latitude. Unit is 8×10^{-4} K · mb s^{-1}.

Table 2. *Energy conversion averaged over the part of the Northern Hemisphere north of 20° N. Values at pressure levels are given in 10^{-3} W m^{-2} mb^{-1}. The vertically integrated conversion has unit W m^{-2}*

	850 mb	500 mb	200 mb	Vertically integrated
Winter	2.01	3.85	0.53	2.13
Spring	2.87	5.86	−1.00	2.58
Summer	0.90	3.42	−0.63	1.23
Fall	1.93	5.44	−0.85	2.17
Year	1.93	4.64	−0.49	2.03

this study compare so well is apparently due to the strong conversion we find in spring and fall. In fact, the semi-annual cycle in the eddy conversion is a very remarkable result. Since this feature occurred in both years (see Fig. 4), it can hardly be attributed to sampling effects. The present material does not allow a sound interpretation of this finding, but a few remarks can be made.

We note from Fig. 3 that the bulk of the conversion takes place at latitudes north of 40° N. This is probably related to the fact that the growth rate of baroclinic waves, for a given meridional temperature gradient, depends on latitude. From a two-dimensional quasi-geostrophic model (e.g. Holton, 1972) we know that the growth rate of the most unstable wave is given by

$$\chi_{\max} = \left[c_1 \left(\frac{\partial T}{\partial y} \right)^2 - c_2 \frac{\beta^2 \sigma^2}{f_o^2} \right]^{1/2} \tag{4}$$

where c_1, c_2 are constants and σ is the static stability. If the expression within the square brackets is negative, no unstable waves exist. From eq. (4) we may get a first impression of how baro-

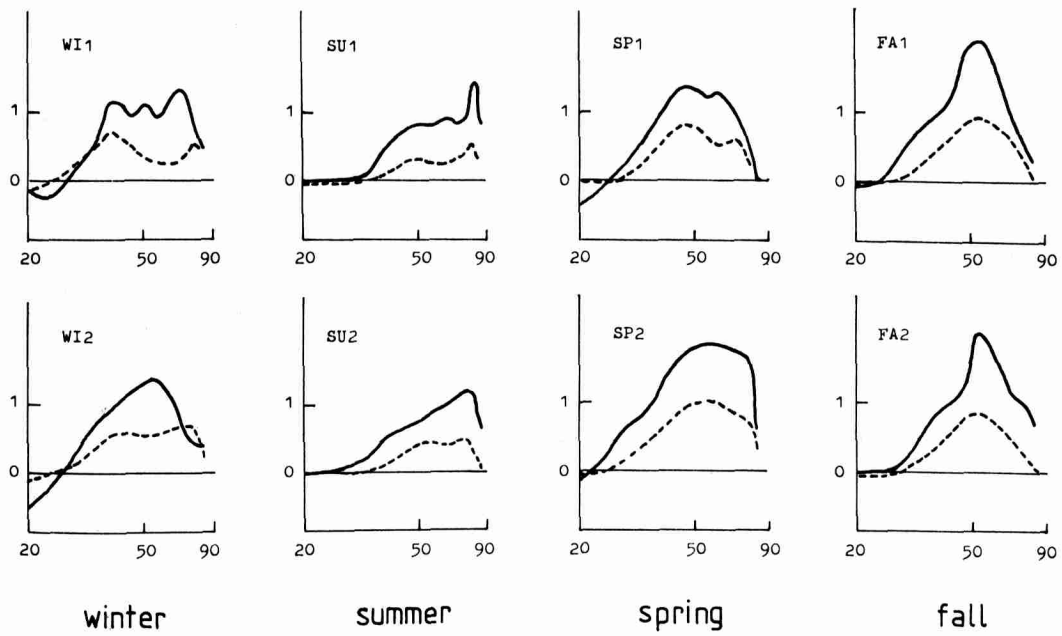

Fig. 4. Values of $\langle \overline{\omega' T'} \rangle$ (solid) and $\langle \overline{v' T'} \rangle$ (dashed) as a function of latitude for all 30-day periods. Units are -10^{-3} K · mb s^{-1} and 10 K · m s^{-1}, respectively.

clinic wave activity depends on latitude. The β-effect decreases polewards whereas f increases. So due to the rotation of the earth, baroclinic development is favoured in higher latitudes. The static stability also plays an important role. It tends to suppress deepening of baroclinic disturbances at the fringes of the sub-tropical high pressure cells. Summarizing, energy conversion by baroclinic eddies, for a given temperature gradient, is likely to be stronger in higher latitudes.

The equator-to-pole temperature gradient, say at 500 mb, shows a smooth annual cycle (Oort and Rasmusson, 1971). It reaches maximum and minimum values in winter and summer, respectively. Inspection of the meridional temperature gradient at middle latitudes, defined as $\Delta T = T_{40°} - T_{70°}$ at 500 mb, brings to light that ΔT reaches maximum values in the transition seasons. Table 3 lists values of ΔT corresponding to the data sample used in this study and the much larger sample used by Oort and Rasmusson (1971), together with the hemispheric energy conversion. Apparently, a semi-annual cycle in ΔT is present. In connection with the remark made in the foregoing paragraph, this offers a possible explanation for the semi-annual cycle in the hemispheric energy conversion by transient eddies. Finally, it is noteworthy that in the energy-budget calculations of Oort and Peixoto (1974), the conversion from transient eddy to mean kinetic energy shows a clear semi-annual cycle with maxima in fall and spring.

5. Relation between $\langle \overline{\omega' T'} \rangle$ and $\langle \overline{v' T'} \rangle$

In zonal statistical-dynamical climate models, a reliable parameterization of the vertical and horizontal eddy heat flux is of crucial importance. A relation frequently referred to is

$$\langle \overline{\omega' T'} \rangle = \mu(\varphi) \langle \overline{v' T'} \rangle \tag{5}$$

Saltzman and Vernekar (1971) derived this relation from a baroclinic instability theory argument. The constant of proportionality $\mu(\varphi)$ is given by the slope of the isentropic surfaces with respect to pressure $[(\partial_p/\partial_y)_\theta]$. Hantel and Baader (1976) find (5) as the first approximation to a more general equation for the upward sensible heat flux. Employing quasi-geostrophic turbulence theory, Sasamori and Melgarejo (1978) also arrived at (5), with $\mu(\varphi) = cf^2/N^2$ (N is the Brunt-Väisälä frequency, c some constant).

Up to now, the parameterization given by (5) has hardly been tested against observations. The present material, however, provides a good opportunity. The relation between the upward and northward heat flux may be considered both with respect to latitude and the seasonal cycle. The latter may be seen as a test where different external forcing is applied to the climate system. If the parameterization holds for the seasonal cycle, it may be used with some confidence in climate-sensitivity studies.

Fig. 4 shows $\langle \overline{\omega' T'} \rangle$ and $\langle \overline{v' T'} \rangle$ at 500 mb for all 30-day periods as a function of latitude. The similarity between both fluxes is striking, though somewhat weaker in winter. Table 4 lists proportionality constants and correlation coefficients between the fluxes. Correlation coefficients are large, but the ratio of the fluxes shows considerable variability.

We shall now observe whether (5) withstands the seasonal cycle. Fig. 5 shows μ obtained by computing the ratio of $\overline{\omega' T'}$ and $\overline{v' T'}$, where *the fluxes were first averaged over the 40–60° N latitude belt.* Again, all data refer to the 500 mb level. The figure

Table 3. *Quantities illustrating the relation between energy conversion and the baroclinicity of the atmosphere. ΔT is defined as the 500 mb temperature difference between 40 and 70° N. O & R stands for Oort and Rasmusson (1971)*

	Total conversion (W/m^2)	ΔT from pres. data (K)	ΔT from O & R, seasons (K)
Winter	2.1	11.4	12.7
Spring	2.6	15.3	14.5
Summer	1.2	10.1	10.5
Fall	2.2	16.1	15.4

Table 4. *Ratio of upward and northward flux of sensible heat and correlation coefficient between those fluxes with respect to latitude* (ρ)

Period	$-\langle\overline{\omega' T'}\rangle \cdot 10^4/\langle\overline{v' T'}\rangle$ (mb/m)	ρ
WI1	2.94	0.779
WI2	2.66	0.884
SP1	2.03	0.963
SP2	1.93	0.953
SU1	2.81	0.987
SU2	2.18	0.955
FA1	2.01	0.975
FA2	2.20	0.959

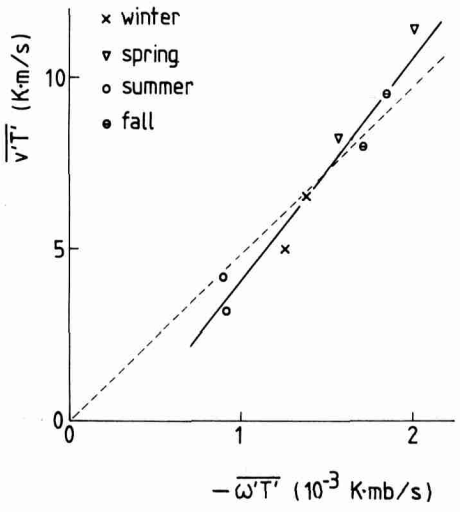

Fig. 5. A plot of $-\overline{\omega' T'}$ vs. $\overline{v' T'}$ at 500 mb, both averaged over the 40–60° N latitude belt. The solid line shows a linear regression, the dashed line one that is forced to go through the origin.

suggests that the ratio of upward and northward heat flux is rather constant through the seasons. We thus have found observational evidence for the universality of (5) as expected from theory. The linear regression shown in Fig. 5 (solid line) is given by

$$-\overline{\omega' T'} = 1.55 \times 10^{-4} \times \overline{v' T'} + 3.72 \times 10^{-4} \quad \text{K} \cdot \text{mb/s}, \tag{6}$$

so $\mu = -1.55 \times 10^{-4}$ mb/m.

At this point some inconsistency shows up. The value of μ suggested by Table 4 is roughly 30% larger than that just derived. This is due to the fact that small values of $\overline{\omega' T'}$ do not occur in Fig. 5. If we force the regression line to go through the origin we find $\mu = -2.12 \times 10^{-4}$ mb/m (dashed line in Fig. 5), which is in better agreement with Table 4.

A comparison of μ with the slope of isentropic surfaces is now in order. Hantel and Baader (1976) computed zonal and annual mean values of $(\partial p/\partial y)_\theta$ from the data of the MIT library. From their Fig. 1 it is seen that $(\partial p/\partial y)_\theta \simeq -10^{-4}$ mb/m for the 40–60° N latitude belt. So, according to the present material, using for μ the annual mean slope of the isentropic surfaces underestimates the upward flux of sensible heat by a factor 1.5 to 2. The results of Sasamori and Melgarejo (1978), after conversion to the p-system, yields $\mu = -1.8 \times 10^{-4}$ mb/m if $f = 10^{-4}$ s^{-1} and $N = 2 \times 10^{-2}$ s^{-1}. This is in good agreement with our quasi-observational results.

6. Discussion

Since the data set used was rather small, we may expect the geographical distributions of $\overline{\omega' T'}$ for the seasons to possess considerable uncertainty. Zonally averaged values, however, appear to be rather stable in view of the similarity between 30-day periods from the same season.

The most striking result of this study is the semi-annual cycle appearing in the hemispheric energy conversion by transient eddies. As already mentioned, there might be a connection with the semi-annual cycle in the conversion of eddy kinetic energy to kinetic energy of the mean flow but conclusions are difficult to draw. The present results clearly show that one should be careful in describing the general circulation by summertime and wintertime conditions with fall and spring "somewhere in between".

The parameterization of $\langle\overline{\omega' T'}\rangle$ in terms of $\langle\overline{v' T'}\rangle$ as proposed by several authors is strongly supported by our findings. Putting those fluxes proportional to each other with a proportionality constant of -1.75 mb/m (at 500 mb) should be sufficiently accurate to simulate both the φ-dependence and the seasonal cycle of $\langle\overline{\omega' T'}\rangle$ in a zonal statistical-dynamical model. According to the present results, choosing for the proportionality

constant the slope of isentropic surfaces underestimates the upward sensible heat flux considerably. We should recall, however, that the proposed parameterizations are based on adiabatic considerations, which means that the only source for eddy potential (and, ultimately, kinetic) energy is the mean potential energy. But in the forecast model used to compute the vertical motion fields, diabatic effects may form a direct source for eddy potential energy. A well-known example is latent heat release in midlatitude storms. Without doubt radiative effects also play their role. It would be very interesting to see how large the "diabatic contribution" to the generation of eddy potential energy is. In practice, however, it will probably be very difficult to separate it from the "adiabatic contribution" in a reliable way.

7. Acknowledgements

All calculations were carried out during a visit of the author to NCAR in fall 1978. I thank Karla Nolan, Ron Madden, Harry van Loon and Paul Mulder for their great help. I also thank my colleagues at the Royal Netherlands Meteorological Institute for their useful comments on an earlier version of this paper. This research was partly supported by NCAR, which is sponsored by the National Science Foundation (U.S.A.).

REFERENCES

Berggren, R. and Nyberg, E. 1967. Eddy vertical transports of latent and sensible heat. *Tellus 19*, 18–23.

Hantel, M. 1976. On the vertical eddy transports in the northern atmosphere. 1. Vertical eddy heat transport for summer and winter. *J. Geoph. Res. 81*, 1577–1588.

Hantel, M. and Baader, H.-R. 1976. On the vertical eddy heat flux in the northern atmosphere. *Beitr. Phys. Atmos. 49*, 149–167.

Holopoainen, E. O. 1963. On the dissipation of kinetic energy in the atmosphere. *Tellus 15*, 26–32.

Holton, J. R. 1972. *An introduction to dynamic meteorology*. Academic Press, 319 pp.

Kung, E. C. 1972. A scheme for kinematic estimate of large-scale vertical motion with an upper-air network. *Quart. J. R. Met. Soc. 98*, 402–411.

Lau, N.-C. 1979. On the structure and energetics of transient disturbances in the Northern Hemisphere wintertime circulation. *J. Atmos. Sci. 36*, 982–995.

Oort, A. H. and Peixóto, J. P. 1974. The annual cycle of the energetics of the atmosphere on a planetary scale. *J. Geoph. Res. 79*, 2705–2719.

Oort, A. H. and Rasmusson, E. 1971. *Atmospheric circulation statistics*. NOAA Prof. Paper No. 5, 323 pp.

Saltzman, B. and Vernekar, A. D. 1971. An equilibrium solution for the axially symmetric component of the earth's macroclimate. *J. Geoph. Res. 76*, 1489–1524.

Sasamori, T. and Melgarejo, J. W. 1978. A parameterization of large-scale heat transport in midlatitudes. Part 1. Transient eddies. *Tellus 30*, 289–299.

Shuman, F. G. and Hovermale, J. B. 1968. An operational six-layer primitive equation model. *J. Appl. Meteor. 7*, 525–547.

ИЗУЧЕНИЕ НАПРАВЛЕННОГО ВВЕРХ ПОТОКА ОЩУТИМОЙ ТЕПЛОТЫ БЛАГОДАРЯ ПЕРЕМЕЩАЮЩИМСЯ ВОЗМУЩЕНИЯМ СИНОПТИЧЕСКОГО МАСШТАБА НА ОСНОВЕ ДАННЫХ НАБЛЮДЕНИЙ

Для восьми 30-дневных периодов, по два в каждом сезоне, на поверхностях 850, 500 и 200 мб рассчитывались вертикальные вихревые потоки тепла из-за движущихся возмущений. Использовались данные анализа Национального метеорологического центра и 6-часовые прогнозы поля ω, проводимые дважды в сутки.

Вертикальные потоки тепла велики на траекториях штормов в Атлантике и Тихом океане и над Скандинавией и Канадой. Интенсивность превращений потенциальной энергии в кинетическую (что прямо связано с вертикальным потоком ощутимой теплоты) перемещающимися возмущениями синоптического масштаба, осредненная по всей атмосфере к северу от 20° с.ш., выявляет максимум весной (2,6 Вт $м^{-2}$) и осенью (2,2 Вт $м^{-2}$). Летом и зимой интенсивности превращений меньше (1,2 и 2,1 Вт $м^{-2}$, соответственно). Средняя за год скорость превращений равна 2,0 Вт $м^{-2}$, что находится в хорошем согласии с величиной 2,2 Вт $м^{-2}$, полученной Оортом и Пейшото (1974). Однако их оценка включает и стационарные вихри.

Найдено, что зонально осредненные вертикальные и меридиональные потоки ощутимой теплоты сильно связаны. Параметризация $\overline{\omega'T'} = \mu\overline{v'T'}$ проверена как по широте, так и по сезону. Представляется что она работает вполне хорошо с величиной μ от $-1{,}5$ до -2 на 10^{-4} м $мб^{-1}$.